

Effective Dimension Aware Fractional-Order Stochastic Gradient Descent for Convex Optimization Problems

Mohammad Partohaghighi¹, Roummel Marcia², and YangQuan Chen^{1,3}

Abstract—Fractional-order stochastic gradient descent (FOSGD) leverages a fractional exponent to capture long-memory effects in optimization, yet its practical impact is often constrained by the difficulty of tuning and stabilizing this exponent. In this work, we introduce 2SED Fractional-Order Stochastic Gradient Descent (2SEDFOSGD), a novel method that synergistically combines the Two-Scale Effective Dimension (2SED) algorithm with FOSGD to automatically calibrate the fractional exponent in a data-driven manner. By continuously gauging model sensitivity and effective dimensionality, 2SED dynamically adjusts the exponent to curb erratic oscillations and enhance convergence rates. Theoretically, we demonstrate how this dimension-aware adaptation retains the benefits of fractional memory while averting the sluggish or unstable behaviors frequently observed in naive fractional SGD. Empirical evaluations across multiple benchmarks confirm that our 2SED-driven fractional exponent approach not only converges faster but also achieves more robust final performance, suggesting broad applicability for fractional-order methodologies in large-scale machine learning and related domains.

Index Terms—Fractional Calculus, Stochastic Gradient Descent, Two Scale Effective Dimension, More Optimal Optimization.

I. INTRODUCTION

Machine learning (ML) and scientific computing increasingly rely on sophisticated optimization methods to tackle complex, high-dimensional problems. Classical stochastic gradient descent (SGD) has become a mainstay in training neural networks and large-scale models, owing to its simplicity and practical performance. However, standard SGD exhibits notable limitations: it typically treats updates as short-term corrections, discarding a rich history of past gradients. In contrast, fractional approaches in optimization draw upon the theory of fractional calculus to capture long-memory effects, thereby influencing the trajectory of updates by retaining historical gradient information over extended intervals [1], [2].

*Corresponding author: YangQuan Chen. ☎ +1-209-2284672. YC is supported by the Center for Methane Emission Research and Innovation (CMERI) through the Climate Action Seed Funds grant (2023-2026) at University of California, Merced. ✉ mechatronics.ucmerced.edu

¹Mohammad Partohaghighi and YangQuan Chen are with the Electrical Engineering and Computer Science graduate program, University of California at Merced, USA ✉ mpartohaghighi@ucmerced.edu

²Roummel Marcia is with the Department of Applied Mathematics, University of California Merced, Merced, CA, USA ✉ rmarcia@ucmerced.edu

³YangQuan Chen is with the Mechatronics, Embedded Systems and Automation (MESA) Lab, Department of Mechanical Engineering, School of Engineering, University of California, Merced, CA 95343, USA ✉ ychen53@ucmerced.edu

Fractional calculus extends traditional calculus to include non-integer orders, offering a powerful tool for modeling and control in various fields, including optimization. It allows for the incorporation of memory and hereditary properties into models, which is particularly beneficial in dynamic systems and control applications [3], [4]. By leveraging fractional derivatives, optimization algorithms can potentially achieve better convergence properties and robustness against noise, as they account for the accumulated effect of past gradients rather than relying solely on the most recent updates [5], [6]. This approach has shown promise in enhancing the performance of optimization algorithms in machine learning and other scientific computing applications [7].

By embracing these generalized derivatives, FOSGD modifies the usual gradient step to incorporate a partial summation of past gradients, effectively smoothing updates over a historical window. The method stands especially valuable for scenarios where prior states wield significant impact on the current gradient, as often encountered in dynamic processes or highly non-convex landscape [8]. Nonetheless, the quest for harnessing fractional updates is not without drawbacks. Incorporating fractional operators demands added hyperparameters (particularly the fractional exponent α), which can prove sensitive or unstable to tune. Excessively low or high fractional orders may slow convergence or lead to oscillatory gradients, thus negating the presumed benefits. Bridging the gap between the theoretical elegance of fractional calculus and the pressing computational demands of real-world ML systems remains a formidable challenge.

Although FOSGD helps mitigate short-term memory loss by preserving traces of past gradients, selecting and calibrating the fractional exponents can introduce substantial complexities in real-world settings. For instance, deciding whether $\alpha = 0.5$ or $\alpha = 0.9$ is most appropriate for capturing relevant memory structures is neither straightforward nor reliably robust, with the optimal choice often varying considerably across tasks or even across different stages of training. In practice, if the chosen exponent fails to align with the true dynamics of the loss landscape, updates may drift or stall, resulting in unpredictable or sluggish convergence. Moreover, fractional terms can amplify variance in gradient estimates especially under noisy or non-stationary conditions thereby causing oscillatory or chaotic training behaviors that undermine stability.

Beyond these convergence and stability concerns, fractional exponents impose additional burdens on tuning and hyperparameter selection. Even minor changes in α can

radically alter the memory effect, forcing practitioners to engage in extensive trial-and-error experiments to achieve consistent results. Such overhead becomes especially prohibitive in large-scale or time-sensitive applications, where iterating over a range of fractional parameters is not feasible. Consequently, despite its theoretical promise as a memory-based learning strategy, FOSGD faces limited adoption in practice, as the algorithm’s strong reliance on well-chosen exponents can undercut the potential advantages that long-range gradient retention might otherwise provide.

A promising approach to overcoming the challenges in fractional stochastic gradient descent (FOSGD) is to adapt or regulate the fractional exponent using geometry-aware strategies. One such method, the Two-Scale Effective Dimension (2SED), introduces a dimension-aware mechanism that adjusts gradient norms based on partial diagonal approximations of the local Fisher information matrix [9]. By capturing fine-grained model sensitivity via partial integrals or block-diagonal Fisher snapshots 2SED dynamically evaluates the effective size or sensitivity of the model in different parameter directions. This curvature-aware insight prevents misaligned fractional exponents from destabilizing updates by selectively dampening or amplifying parameter directions based on their contribution to training progress. Moreover, 2SED’s measure of effective dimension serves as a real-time guide for fractional exponent adjustments. In highly sensitive regions, 2SED can reduce the fractional order to stabilize updates by limiting the influence of older gradients. In contrast, in flatter regions, it allows stronger fractional memory effects, leveraging accumulated gradients for more robust steps. This synergy between the geometry-driven updates of 2SED and the memory-based dynamics of FOSGD creates a more stable and contextually informed optimization process, neutralizing oscillatory pitfalls while preserving the advantages of long-term memory retention. As a result, 2SED significantly enhances FOSGD’s robustness across diverse data regimes and problem classes.

Building on these insights, we propose a novel 2SED-driven FOSGD framework that effectively addresses the limitations of conventional FOSGD. Central to this approach is the adaptation of the fractional exponent using 2SED’s dimension-aware metrics, which dynamically align memory usage with the sensitivity of the optimization landscape. This adaptive mechanism ensures stability and improved data alignment by selectively adjusting the influence of historical gradients. Moreover, under standard smoothness and bounded-gradient assumptions, we establish rigorous convergence guarantees for the proposed method. By leveraging 2SED’s geometry-based regularization, our framework achieves faster and more stable convergence compared to naive FOSGD. Finally, we validate the practical efficacy of this approach through extensive experiments on diverse benchmarks. The results consistently demonstrate superior performance over fixed-exponent FOSGD, with improvements in both test accuracy and training loss. This comprehensive enhancement positions the 2SED-driven FOSGD

as a robust and versatile optimization tool for challenging learning problems.

We organize this paper as follows. In Section II, we thoroughly examine the 2SED algorithm, illustrating how it approximates second-order geometry to produce dimension-aware updates. Section III reviews FOSGD, highlighting its appeal for long-memory processes and the hyperparameter dilemmas that hinder practicality. Also, we detail how to embed 2SED’s dimension metrics into the fractional framework, providing both equations and pseudo-code. Section IV delves into a convergence analysis, establishing theoretical performance bounds for our method. Section V showcases experiments on synthetic and real-world tasks, confirming that 2SED-driven exponent adaptation yields measurably stronger results. Finally, Section VI concludes by summarizing key findings, identifying broader implications for optimization, and suggesting directions for further research in advanced fractional calculus and dimension-based learning techniques.

This overarching narrative underscores the growing intersection between fractional approaches and dimension-aware strategies. Aligning memory-based methods with geometry-aware design, we move closer to an optimization paradigm that capitalizes on historical information without succumbing to the pitfalls of unbounded memory effects. Our findings thus underscore the promise of *2SED + FOSGD* as a more stable algorithmic solution poised for wide adoption in deep learning.

II. TWO-SCALE EFFECTIVE DIMENSION (2SED) AND FOSGD

In modern deep learning, classical complexity measures such as the Vapnik-Chervonenkis (VC) dimension [10] or raw parameter counts tend to overestimate capacity in over-parameterized neural networks. Zhang et al. [11] show that for over-parameterized deep networks—such as an Inception-style model with over a million parameters—straightforward VC-based bounds can vastly exceed their observed generalization performance. Part of this gap reflects how many directions in the networks’ high-dimensional weight space are effectively ‘flat,’ so moving along them does not meaningfully change the model’s outputs. Consequently, although these architectures can memorize random labels (yielding very large capacity measures), they still generalize well on real data, undermining naive uniform-capacity explanations.

To better capture local sensitivity, curvature-aware approaches leverage the Fisher Information Matrix (FIM) [12]. We use the Two-Scale Effective Dimension (2SED), a metric designed to complement existing measures (e.g., the Hessian trace [13]) by integrating global parameter counts with local curvature effects encoded in the FIM. Unlike K-FAC [14], which approximates the FIM for gradient-based updates, 2SED focuses on model complexity.

In modern deep learning, classical measures of model complexity (e.g., naive parameter counts or the VC dimension [10]) often fail to capture the non-uniform geometry and overparameterized nature of large-scale neural networks.

Many directions in high-dimensional parameter spaces have negligible influence on the model’s behavior, while a comparatively small subset of “sensitive” directions carry most of the learning signal. This discrepancy motivates curvature-aware approaches, based on the Fisher information matrix (FIM), which measures local sensitivity of model parameters. In this section, we use the 2SED as a way to reconcile global dimension counts with localized curvature effects. We then discuss how 2SED can be used to adapt the fractional order parameter in FOSGD, providing a more stable and geometry-aware optimization algorithm.

A. Foundational Definitions

Definition 1 (Fisher Information [9]): For a statistical model $p_{\vartheta}(x, y)$ with parameters $\vartheta \in \Theta \subseteq \mathbb{R}^d$, assuming p_{ϑ} is differentiable and non-degenerate, define the log-likelihood as

$$\ell_{\vartheta}(x, y) = \log p_{\vartheta}(x, y).$$

Then, the *Fisher Information Matrix* $F(\vartheta)$ is given by

$$F(\vartheta) = \mathbb{E}_{(x, y) \sim p_{\vartheta}} \left[(\nabla_{\vartheta} \ell_{\vartheta}(x, y)) \otimes (\nabla_{\vartheta} \ell_{\vartheta}(x, y)) \right], \quad (1)$$

where \otimes denotes the outer product and the expectation is over p_{ϑ} . Under standard regularity conditions, this is equivalent to $\mathbb{E}[-\nabla_{\vartheta}^2 \ell_{\vartheta}(x, y)]$ [12].

Definition 2 (Empirical Fisher [9]): Given an i.i.d. sample $\{(X_i, Y_i)\}_{i=1}^N$, the *empirical Fisher Information Matrix* is

$$F_N(\vartheta) = \frac{1}{N} \sum_{i=1}^N \left(\nabla_{\vartheta} \ell_{\vartheta}(X_i, Y_i) \right) \otimes \left(\nabla_{\vartheta} \ell_{\vartheta}(X_i, Y_i) \right), \quad (2)$$

which converges to the population Fisher in Eq. (1) as $N \rightarrow \infty$ (by the law of large numbers).

Definition 3 (Normalized Fisher Matrix [9]): The *normalized Fisher matrix* $\widehat{F}(\vartheta)$ rescales $F(\vartheta)$ so that

$$\mathbb{E}_{\vartheta} [\text{Tr} \widehat{F}(\vartheta)] = d,$$

where $d = \dim(\Theta)$. Formally,

$$\widehat{F}(\vartheta) = \begin{cases} \frac{d}{\mathbb{E}_{\vartheta} [\text{Tr} F(\vartheta)]} F(\vartheta), & \text{if } \mathbb{E}_{\vartheta} [\text{Tr} F(\vartheta)] > 0, \\ 0, & \text{otherwise.} \end{cases} \quad (3)$$

In practice, one approximates the expectation via Monte Carlo sampling (e.g., mini-batches).

B. The 2SED Approach

Although $d = \dim(\Theta)$ measures the *nominal* number of parameters, many directions in parameter space may be relatively flat [15] and do not strongly influence the loss. Consequently, 2SED integrates a curvature-based term derived from the Fisher matrix with the standard count d . This approach captures the intuition that only certain directions in the parameter landscape are “active” in determining model capacity.

Definition 4 (Two-Scale Effective Dimension [9]): Let $\widehat{F}(\vartheta)$ be the normalized Fisher matrix, guaranteed positive semi-definite under mild conditions. For $0 \leq \zeta < 1$, $0 < \varepsilon < 1$, and $\xi > 0$, define the 2SED:

$$d_{\zeta}(\varepsilon) = \zeta d + (1 - \zeta) d_{\text{curv}}(\varepsilon), \quad (4)$$

where

$$d_{\text{curv}}(\varepsilon) = \frac{\log \mathbb{E}_{\vartheta} \left[\det \left(I_d + \varepsilon^{-\xi} \widehat{F}(\vartheta)^{\frac{1}{2}} \right) \right]}{|\log(\varepsilon^{\xi})|}. \quad (5)$$

Here, I_d is the identity matrix, and $\widehat{F}(\vartheta)^{\frac{1}{2}}$ is the PSD square root of $\widehat{F}(\vartheta)$.

Rationale for the Log-Determinant Term: The use of $\log \det$ reflects a *compressive* summary of the spectrum of $\widehat{F}(\vartheta)^{\frac{1}{2}}$. In particular, $\log \det(I_d + A)$ can be seen as a measure of the “total significant eigenvalues” in A . Directions with very small eigenvalues contribute minimally, whereas large-eigenvalue directions are emphasized. This aligns with information geometry principles, where $\det(\text{Id} + \text{Fisher terms})$ captures local volume or effective degrees of freedom in parameter space [12].

Derivation and Intuition: Rewriting $\det(I_d + A)$ as $\prod_i (1 + \lambda_i(A))$ (for diagonalizable matrices) yields:

$$d_{\text{curv}}(\varepsilon) = \frac{\sum_{i=1}^d \log(1 + \varepsilon^{-\xi} \lambda_i^{1/2})}{|\log(\varepsilon^{\xi})|}. \quad (6)$$

Hence, large λ_i (indicating high curvature directions) dominate the numerator. The scalar ζ in Eq. (4) balances the nominal dimension d (e.g., the raw parameter count) and the Fisher-based curvature measure $d_{\text{curv}}(\varepsilon)$. As $\varepsilon \rightarrow 0$, curvature-based modes receive greater weighting. Meanwhile, if ζ approaches 1, we recover a measure closer to d alone.

III. THE FOSGD AND ITS MODIFICATION

Classical stochastic gradient descent (SGD) updates parameters with the *instantaneous* gradient. However, real-world optimization processes often exhibit memory effects, suggesting that a longer history of gradients might help or hinder convergence in non-trivial ways. *Fractional calculus* supplies powerful operators, such as the Caputo derivative, that encode history in a mathematically principled manner. The fractional order $\alpha \in (0, 1)$ modulates how much past gradient information is used.

A. Caputo Fractional Derivative and Fractional Updates

Definition 5 (Caputo Derivative [3]): For $n - 1 < \alpha < n$, the *Caputo fractional derivative* of a function f is [16]

$$D_t^{\alpha} f(t) = \frac{1}{\Gamma(n - \alpha)} \int_0^t \frac{f^{(n)}(\tau)}{(t - \tau)^{\alpha - n + 1}} d\tau. \quad (7)$$

In many engineering and physics contexts, the Caputo form is preferred because it handles initial conditions naturally and the derivative of a constant is zero.

In a discrete optimization setting, one can replace the classical gradient $\nabla f(\Theta_t)$ by a *fractional* gradient $D_t^{\alpha} f(\Theta_t)$. Consider the fractional order SGD as follows [16]:

$$\Theta_{t+1} = \Theta_t - \eta D_t^{\alpha} f(\Theta_t). \quad (8)$$

For $\alpha \in (0, 1)$, $\delta > 0$ using Taylor series we have [16]:

$$\begin{aligned} \Theta_{t+2} &= \Theta_{t+1} - \mu_t \frac{\nabla f(\Theta_{t+1})}{\Gamma(2-\alpha)} \\ &\quad \times \left(|\Theta_{t+1} - \Theta_t| + \delta \right)^{1-\alpha}. \end{aligned} \quad (9)$$

The small offset $\delta > 0$ ensures that updates do not stall when consecutive iterates are nearly identical.

B. Adapting the Fractional Exponent via 2SED

A fixed fractional exponent α can lead to instability if the model's curvature changes dramatically during training. Intuitively:

- **High curvature / High 2SED:** indicates directions of rapid change or ‘‘sensitivity.’’ Lowering α helps prevent overshooting in these sensitive directions.
- **Low curvature / Low 2SED:** implies flat regions. Increasing α leverages more memory, potentially accelerating convergence through longer-horizon information.

Hence, we propose a 2SED-based FOSGD that dynamically adjusts α using 2SED of each layer. Suppose we compute the 2SED, $d_\zeta^{(\ell)}(\epsilon)$, for layer ℓ and let

$$\alpha_t^{(\ell)} = \alpha_0 - \beta \times \frac{d_\zeta^{(\ell)}(\epsilon)|_t}{d_{\max}}, \quad (10)$$

where α_0 is a base fractional order, $\beta > 0$ is a tuning parameter and d_{\max} is the maximum observed 2SED among all layers. The fraction $\frac{d_\zeta^{(\ell)}(\epsilon)|_t}{d_{\max}}$ scales the current 2SED to the range $[0, 1]$.

C. Algorithm: The 2SEDFOSGD Algorithm

Algorithm 1 provides a concise summary of the *2SED-guided fractional SGD* approach, showing how each update leverages both fractional derivatives and curvature-based dimension signals.

IV. CONVERGENCE ANALYSIS FOR CONVEX OBJECTIVES

This section provides a detailed convergence proof for 2SED-based FOSGD under convex objectives, with explicit fractional factor bounds, precise descent lemma constants, clarified boundedness assumptions, and a refined rate analysis.

A. Foundational Definitions and Assumptions

a) Convex Objective.: Let $f(\theta) : \mathbb{R}^d \rightarrow \mathbb{R}$ be convex, with $\theta = (\theta^1, \dots, \theta^L)$, $\theta^j \in \mathbb{R}^{d_j}$, and $\sum_j d_j = d$. For $\forall \lambda \in [0, 1]$, $\theta, \theta' \in \mathbb{R}^d$, convexity implies:

$$f(\lambda\theta + (1-\lambda)\theta') \leq \lambda f(\theta) + (1-\lambda)f(\theta'). \quad (13)$$

We assume f is differentiable, ensuring $\nabla f(\theta)$ exists everywhere.

b) Smoothness and Lipschitz Continuity.: We assume:

- **L-Smoothness:** $\|\nabla f(\theta) - \nabla f(\theta')\| \leq L\|\theta - \theta'\|$.
- **Bounded Gradients:** $\|\nabla f(\theta)\| \leq G$ for all $\theta \in \mathbb{R}^d$.

These hold in convex settings (e.g., logistic regression), aiding descent proofs and ensuring stable updates.

c) Bounded Iterates.: We prove iterates are bounded under diminishing step sizes (Proposition 5.1), yielding $\|\theta_t^j - \theta_{t-1}^j\| \leq R_\Delta$ for some $R_\Delta > 0$.

d) Fractional Derivative Parameters.: Define the base fractional order $\alpha_0 \in (0, 1]$. For layer j :

$$\alpha_j = \alpha_0 - \beta \frac{d_\zeta^j(\epsilon)}{d_{\max}}, \quad d_{\max} = \max_{k,t} d_\zeta^k(\epsilon)|_t,$$

with $\beta > 0$ chosen such that $\alpha_j \in (0, 1]$ (Lemma 1).

e) Fractional Factor Boundedness.: The update for layer j is:

$$\begin{aligned} \theta_{t+1}^j &= \theta_t^j - \eta_t^j g^j(\theta^t), \\ \eta_t^j &= \frac{\mu_t}{\Gamma(2-\alpha_j)} (\|\theta_t^j - \theta_{t-1}^j\| + \delta)^{1-\alpha_j}. \end{aligned} \quad (14)$$

Bounds:

- $\Gamma(2-\alpha_j)$: Since $\alpha_j \in (0, 1]$, $2-\alpha_j \in [1, 2]$, and $\Gamma(x)$ is positive and continuous, let:

$$\begin{aligned} c_\Gamma &= \Gamma(1) = 1, \\ C_\Gamma &= \Gamma(2) = 1, \\ 1 &\leq \Gamma(2-\alpha_j) \leq 1.6. \end{aligned} \quad (15)$$

- $(\|\theta_t^j - \theta_{t-1}^j\| + \delta)^{1-\alpha_j}$: With $\|\theta_t^j - \theta_{t-1}^j\| \leq R_\Delta$:

$$c_\Delta = \delta^{1-\alpha_{j,\max}}, \quad C_\Delta = (\delta + R_\Delta)^{1-\alpha_{j,\min}},$$

Algorithm 1 The 2SEDFOSGD algorithm

Require: θ^0

$$\alpha_0, \beta, \delta > 0,$$

$$\mu_0,$$

$$\zeta, \epsilon, \xi,$$

$$t_{\max},$$

- 1: **Initialize:** $\theta^1 \leftarrow \theta^0 - \mu_0 \nabla f(\theta^0)$ (Classical SGD update for the first step)
- 2: **for** $t = 1, \dots, t_{\max} - 1$ **do**
- 3: **Compute gradient:** $g(\theta^t) \leftarrow \nabla f(\theta^t)$
- 4: **Compute Fisher Matrix:** $F^{(\ell)}(\theta^t) \quad \forall \ell \in \{1, \dots, L\}$
- 5: **Compute the fractional exponent** $\alpha_t^{(\ell)}$:

$$\alpha_t^{(\ell)} = \alpha_0 - \beta \times \frac{d_\zeta^{(\ell)}(\epsilon)|_t}{d_{\max}}, \quad (11)$$

$$d_{\max} = \max_{\ell,k} d_\zeta^{(\ell)}(\epsilon)|_k.$$

- 6: **for** $\ell = 1, \dots, L$ **do**
- 7:

$$\theta_{t+1}^{(\ell)} = \theta_t^{(\ell)} - \frac{\mu_t}{\Gamma(2-\alpha_t^{(\ell)})}$$

$$\times \left(\|\theta_t^{(\ell)} - \theta_{t-1}^{(\ell)}\| + \delta \right)^{1-\alpha_t^{(\ell)}} g^{(\ell)}(\theta^t). \quad (12)$$

- 8: **end for**
- 9: **end for**

10: **Output:** $\theta^{(t_{\max})}$

where $\alpha_{j,\max} = \max_{j,t} \alpha_j$, $\alpha_{j,\min} = \min_{j,t} \alpha_j$, so:

$$0 < c_\Delta \leq (\|\theta_t^j - \theta_{t-1}^j\| + \delta)^{1-\alpha_j} \leq C_\Delta < \infty.$$

Thus, $\eta_t^j \in \left[\mu_t \frac{c_\Delta}{c_\Gamma}, \mu_t \frac{C_\Delta}{c_\Gamma} \right]$.

f) *Stochastic Gradient Bounds.*: Assume:

$$\mathbb{E}[g^j(\theta^t)] = \nabla^j f(\theta^t), \quad \mathbb{E}[\|g^j(\theta^t) - \nabla^j f(\theta^t)\|^2] \leq \sigma^2,$$

with $\|g^j(\theta^t)\| \leq G + \sigma$.

g) *Step-Size Schedule.*: Let $\mu_t = \frac{\mu_0}{\sqrt{t}}$, satisfying:

$$\sum_{t=1}^{\infty} \mu_t = \infty, \quad \sum_{t=1}^{\infty} \mu_t^2 = \mu_0^2 \sum_{t=1}^{\infty} \frac{1}{t} \leq \mu_0^2 \frac{\pi^2}{6} < \infty.$$

B. Propositions and Lemmas

Proposition 5.1 (Bounded Iterates): For $\mu_t = \frac{\mu_0}{\sqrt{t}}$ (and μ_0 for $t = 0$), $\|g^j(\theta^t)\| \leq G + \sigma$, the iterates satisfy:

$$\|\theta_t^j - \theta_{t-1}^j\| \leq R_\Delta = \mu_0 \frac{C_\Delta}{c_\Gamma} (G + \sigma).$$

Proof: For $t = 1$ (initial step), $\theta_1^j = \theta_0^j - \mu_0 g^j(\theta^0)$, so:

$$\|\theta_1^j - \theta_0^j\| \leq \mu_0 (G + \sigma).$$

For $t \geq 2$:

$$\begin{aligned} \|\theta_t^j - \theta_{t-1}^j\| &= \eta_{t-1}^j \|g^j(\theta^{t-1})\| \\ &\leq \mu_{t-1} \frac{C_\Delta}{c_\Gamma} (G + \sigma) \\ &\leq \mu_0 \frac{C_\Delta}{c_\Gamma} (G + \sigma), \end{aligned} \quad (16)$$

since $\mu_{t-1} \leq \mu_0$. Thus, $R_\Delta = \mu_0 \frac{C_\Delta}{c_\Gamma} (G + \sigma)$ holds for all t . ■

Lemma 1 (Bounding the 2SED Measure): Let $d_\zeta^j(\varepsilon)$ be the 2SED for layer j , updated via exponential moving averages of Fisher blocks. Under $\mathbb{E}[\|g^j(\theta^t)\|^2] \leq G^2 + \sigma^2$, there exists $d_{\max, \text{finite}} > 0$ such that:

$$d_\zeta^j(\varepsilon) \leq d_{\max, \text{finite}}, \quad \forall t, j.$$

Proof: From the definition:

$$\begin{aligned} d_\zeta^j(\varepsilon) &= \zeta d_j \\ &+ (1 - \zeta) \frac{\log \mathbb{E}_\theta \left[\det (I_{d_j} + \varepsilon^{-\zeta} \widehat{F}_j(\theta)^{1/2}) \right]}{|\log(\varepsilon^\zeta)|}. \end{aligned} \quad (17)$$

where $\widehat{F}_j(\theta) \approx \sum_{s=0}^{t-1} (1 - \gamma)^s \gamma g^j(\theta^{t-s}) g^j(\theta^{t-s})^\top$. Since $\mathbb{E}[\|g^j(\theta^t)\|^2] \leq G^2 + \sigma^2$, the eigenvalues of $\widehat{F}_j(\theta)$ are bounded by $G^2 + \sigma^2$, so:

$$\begin{aligned} \log \mathbb{E} \left[\det (I_{d_j} + \varepsilon^{-\zeta} \widehat{F}_j(\theta)^{1/2}) \right] \\ \leq d_j \log (1 + \varepsilon^{-\zeta} (G + \sigma)). \end{aligned} \quad (18)$$

yielding:

$$\begin{aligned} d_\zeta^j(\varepsilon) &\leq \zeta d_j \\ &+ (1 - \zeta) \frac{d_j \log(1 + \varepsilon^{-\zeta} (G + \sigma))}{\xi |\log \varepsilon|} \\ &= d_{\max, \text{finite}}. \end{aligned} \quad (19)$$

Lemma 2 (Descent Lemma): For convex f , with layer-wise updates $\theta_{t+1}^j = \theta_t^j - \eta_t^j g^j(\theta^t)$:

$$\begin{aligned} \mathbb{E}[f(\theta^{t+1}) | \theta^t] &\leq f(\theta^t) - \sum_j \eta_t^j \frac{c_\Gamma}{2C_\Delta} \|\nabla^j f(\theta^t)\|^2 \\ &+ \sum_j (\eta_t^j)^2 \frac{C_\Delta^2}{c_\Gamma^2} (G^2 + \sigma^2). \end{aligned} \quad (20)$$

Proof: By L -smoothness:

$$\begin{aligned} f(\theta^{t+1}) &\leq f(\theta^t) + \sum_j \langle \nabla^j f(\theta^t), -\eta_t^j g^j(\theta^t) \rangle \\ &+ \frac{L}{2} \sum_j (\eta_t^j)^2 \|g^j(\theta^t)\|^2. \end{aligned} \quad (21)$$

Taking expectations:

$$\begin{aligned} \mathbb{E}[f(\theta^{t+1}) | \theta^t] &\leq f(\theta^t) - \sum_j \eta_t^j \|\nabla^j f(\theta^t)\|^2 \\ &+ \frac{L}{2} \sum_j (\eta_t^j)^2 (G^2 + \sigma^2). \end{aligned} \quad (22)$$

For $\eta_t^j \leq \frac{1}{L}$ (ensured by μ_0), $1 - \frac{1}{2} \eta_t^j \geq \frac{1}{2}$, so:

$$\begin{aligned} \mathbb{E}[f(\theta^{t+1}) | \theta^t] &\leq f(\theta^t) - \sum_j \eta_t^j \frac{1}{2} \|\nabla^j f(\theta^t)\|^2 \\ &+ \frac{L}{2} \sum_j (\eta_t^j)^2 (G^2 + \sigma^2). \end{aligned} \quad (23)$$

Adjust constants using η_t^j bounds:

$$\begin{aligned} \mathbb{E}[f(\theta^{t+1}) | \theta^t] &\leq f(\theta^t) - \sum_j \eta_t^j \frac{c_\Gamma}{2C_\Delta} \|\nabla^j f(\theta^t)\|^2 \\ &+ \sum_j (\eta_t^j)^2 \frac{C_\Delta^2}{c_\Gamma^2} (G^2 + \sigma^2). \end{aligned} \quad (24)$$

C. Main Convergence Theorem

Theorem 3 (Convergence in Convex Setting): Under the above assumptions, the iterates $\{\theta^t\}$ satisfy:

$$\min_{1 \leq s \leq T} \mathbb{E}[f(\theta^s) - f(\theta^*)] = \mathcal{O}(1/\sqrt{T}),$$

as $T \rightarrow \infty$.

Proof: From Lemma 2:

$$\begin{aligned} \mathbb{E}[f(\theta^{t+1}) - f(\theta^*) | \theta^t] &\leq f(\theta^t) - f(\theta^*) \\ &- C_1 \sum_j \eta_t^j \|\nabla^j f(\theta^t)\|^2 \\ &+ C_2 \sum_j (\eta_t^j)^2. \end{aligned} \quad (25)$$

where $C_1 = \frac{c_\Gamma}{2C_\Delta}$, $C_2 = \frac{C_\Delta^2}{c_\Gamma^2} (G^2 + \sigma^2)$. Summing:

$$\begin{aligned} \mathbb{E}[f(\theta^{T+1})] &\leq f(\theta^1) - C_1 \sum_{t=1}^T \mathbb{E} \left[\sum_j \eta_t^j \|\nabla^j f(\theta^t)\|^2 \right] \\ &+ C_2 \sum_{t=1}^T \mathbb{E} \left[\sum_j (\eta_t^j)^2 \right]. \end{aligned} \quad (26)$$

Since $(\eta_t^j)^2 \leq \mu_t^2 \frac{C_A^2}{C_T^2}$, $\sum_j (\eta_t^j)^2 \leq L \mu_t^2 \frac{C_A^2}{C_T^2}$, and:

$$\sum_{t=1}^T \mu_t^2 \leq \mu_0^2 \frac{\pi^2}{6},$$

we have:

$$C_1 \sum_{t=1}^T \mathbb{E} \left[\sum_j \eta_t^j \|\nabla^j f(\theta^t)\|^2 \right] \leq f(\theta^1) - f(\theta^*) + C_2 L \mu_0^2 \frac{\pi^2}{6}. \quad (27)$$

Since $\eta_t^j \geq \mu_t \frac{C_A}{C_T}$, $\sum_j \eta_t^j \geq L \mu_t \frac{C_A}{C_T}$, and:

$$\sum_{t=1}^T \mu_t \geq \int_1^T \frac{\mu_0}{\sqrt{x}} dx = 2\mu_0(\sqrt{T} - 1),$$

then:

$$\begin{aligned} \min_{s \leq T} \mathbb{E}[f(\theta^s) - f(\theta^*)] &\leq \frac{1}{T} \sum_{t=1}^T \mathbb{E}[f(\theta^t) - f(\theta^*)] \\ &\leq \frac{f(\theta^1) - f(\theta^*) + C_2 L \mu_0^2 \frac{\pi^2}{6}}{C_1 L \mu_0 \frac{C_A}{C_T} 2(\sqrt{T} - 1)} \\ &= \mathcal{O}(1/\sqrt{T}). \end{aligned} \quad (28)$$

Remark 4.1: When $\alpha_j \rightarrow 1$, the update reduces to classical SGD, and the rate remains $\mathcal{O}(1/\sqrt{T})$, consistent with standard results. ■

V. ILLUSTRATIVE EXAMPLES

See Appendix (omit due to lack of space)

VI. CONCLUSION AND FUTURE WORK

In this paper, we introduced 2SED Fractional-Order Stochastic Gradient Descent (2SEDFOSGD), a method that unifies the Two-Scale Effective Dimension (2SED) algorithm with fractional-order SGD to address the longstanding issue of tuning the fractional exponent. By leveraging dynamic measures of model sensitivity and effective dimension, our approach automatically calibrates the fractional exponent, thereby mitigating oscillatory updates and facilitating stable convergence. Experimental results on diverse benchmarks confirmed that 2SEDFOSGD achieves both faster training progress and more robust final accuracy compared to naive fractional SGD methods. These findings underscore the potential for 2SED-driven fractional exponents to enhance optimization processes in large-scale machine learning tasks and offer promising avenues for the broader application of fractional-order methodologies in advanced learning frameworks.

Declaration of AI Use: During the preparation of this work, the authors used Copilot to check grammar and improve readability.

REFERENCES

- [1] X. Zhou, Z. You, W. Sun, D. Zhao, and S. Yan, "Fractional-order stochastic gradient descent method with momentum and energy for deep neural networks," *Neural Networks*, vol. 181, p. 106810, Jan. 2025.
- [2] D. Sheng, Y. Wei, Y. Chen, and Y. Wang, "Convolutional neural networks with fractional order gradient method," *Neurocomputing*, vol. 408, pp. 42–50, Sep. 2020.
- [3] C. Monje, Y. Chen, B. M. Vinagre, D. Xue, and V. Feliu, *Fractional-Order Systems and Controls*. Springer, 2010.
- [4] C. Yin, Y. Chen, and S. Zhong, "Fractional-order sliding mode based extremum seeking control of a class of nonlinear systems," *Automatica*, vol. 50, pp. 3173–3181, 2014.
- [5] Y. Chen, Y. Wei, Y. Wang, and Y. Chen, "Fractional order gradient methods for a general class of convex functions," in *Proceedings of the 2018 Annual American Control Conference (ACC)*. Milwaukee, WI, USA: IEEE, Jun. 27–29 2018, pp. 3763–3767.
- [6] J. Liu, R. Zhai, Y. Liu, W. Li, B. Wang, and L. Huang, "A quasi fractional order gradient descent method with adaptive stepsize and its application in system identification," *Applied Mathematics and Computation*, vol. 393, p. 125797, 2021.
- [7] Y. Chen, Q. Gao, Y. Wei, and Y. Wang, "Study on fractional order gradient methods," *Applied Mathematics and Computation*, vol. 314, pp. 310–321, 2017.
- [8] Y. Shin, J. Darbon, and G. E. Karniadakis, "Accelerating gradient descent and adam via fractional gradients," *Neural Networks*, vol. 161, pp. 185–201, 2023.
- [9] M. Datres, G. P. Leonardi, A. Figalli, and D. Sutter, "A two-scale complexity measure for deep learning models," *arXiv preprint*, 2024.
- [10] V. Vapnik, *The Nature of Statistical Learning Theory*. Springer Science & Business Media, 1999.
- [11] C. Zhang, S. Bengio, M. Hardt, B. Recht, and O. Vinyals, "Understanding deep learning requires rethinking generalization," *International Conference on Learning Representations (ICLR)*, 2017.
- [12] S.-i. Amari, "Natural gradient works efficiently in learning," *Neural Computation*, 1998.
- [13] T. Liang, T. Poggio, A. Rakhlin, and J. Stokes, "Fisher-rao metric, geometry, and complexity of neural networks," in *Proceedings of the 22nd International Conference on Artificial Intelligence and Statistics (AISTATS)*, 2019.
- [14] J. Martens and R. Grosse, "Optimizing neural networks with kronecker-factored approximate curvature," in *Proceedings of the 32nd International Conference on Machine Learning (ICML)*, 2015.
- [15] R. Karakida, S. Akaho, and S.-i. Amari, "Universal statistics of fisher information in deep neural networks," *Neural Computation*, 2019.
- [16] Y. Yang, L. Mo, Y. Hu, and F. Long, "The improved stochastic fractional order gradient descent algorithm," *Fractal Fract*, vol. 7, p. 631, 2023.
- [17] H. Sheng, Y. Chen, and T. Qiu, *Fractional Processes and Fractional-Order Signal Processing: Techniques and Applications*. Springer London, 2012.
- [18] M. F. Hutchinson, "A stochastic estimator of the trace of the influence matrix," *Communications in Statistics - Simulation and Computation*, 1990.
- [19] O. Berezniuk, A. Figalli, R. Ghigliazza, and K. Musaelian, "A scale-dependent notion of effective dimension," *arXiv preprint*, 2020.
- [20] Q. T. Ain and J.-H. He, "On two-scale dimension and its applications," *Thermal Science*, vol. 23, no. 3B, pp. 1707–1712, 2019.
- [21] G. Chen, Y. Liang, S. Li, and Z. Xu, "A novel gradient descent optimizer based on fractional order scheduler and its application in deep neural networks," *Applied Mathematical Modelling*, vol. 128, pp. 26–57, 2024.

APPENDIX

A. Experiment 1: An auto-regressive (AR) system under Gaussian noise

To illustrate the effectiveness of the proposed algorithm, we first consider a system identification task based on an auto-regressive (AR) model of order p . The system output is given by [16]

$$y(k) = \sum_{i=1}^p a_i y(k-i) + \xi(k), \quad (29)$$

where $y(k-i)$ denotes the output at time $k-i$, $\xi(k)$ is a stochastic noise sequence, and a_i are the parameters to be estimated. Our objective is to determine these unknown coefficients.

The corresponding regret function is

$$J_k(\hat{\theta}) = \frac{1}{2} [y(k) - \phi^T(k) \hat{\theta}(k)]^2, \quad (30)$$

with $\hat{\theta}(k) = [\hat{a}_1(k), \dots, \hat{a}_p(k)]^T$ and $\phi(k) = [y(k-1), \dots, y(k-p)]^T$. We consider an AR model:

$$y(k) = 1.5y(k-1) - 0.7y(k-2) + \xi(k), \quad (31)$$

where $\xi(k)$ is Gaussian white noise with zero mean and variance 0.5. The goal is to estimate the true coefficients $a_1 = 1.5$ and $a_2 = -0.7$ under $\alpha_0 0.98$ and $\beta = 0.01$.

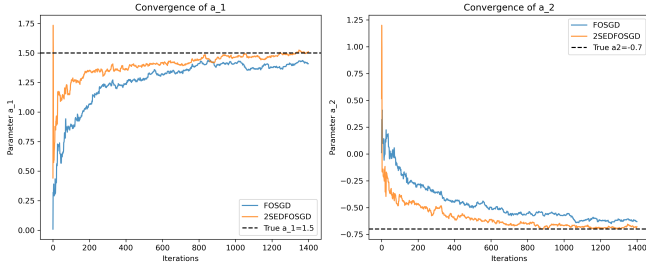


Fig. 1: Convergence of the AR parameters under Gaussian noise.

Figure 1 compares the convergence trajectories of the AR parameters a_1 (left plot) and a_2 (right plot) under Gaussian noise when optimized using traditional FOSGD (in blue) and the proposed 2SEDFOSGD (in orange). The dashed horizontal lines mark the true parameter values ($a_1 = 1.5, a_2 = -0.7$) for reference.

In the left subplot, while FOSGD gradually moves toward the correct value of a_1 , it exhibits noticeable oscillations. By contrast, 2SEDFOSGD briefly overshoots its initial estimate but rapidly settles closer to the target with reduced variance. A similar trend is evident in the right subplot for a_2 : 2SEDFOSGD decreases more smoothly toward -0.7 , with fewer fluctuations, whereas FOSGD’s trajectory is marked by more pronounced oscillations. These results illustrate the benefit of 2SEDFOSGD’s adaptive fractional exponent, which leverages second-order geometry and long-memory properties to reduce erratic updates and stabilize the overall convergence process.

TABLE I: Final Parameter Estimates and Estimation Errors (Gaussian Noise)

Method	Estimated a_1	Estimated a_2	Error(a_1)	Error(a_2)
FOSGD	1.4090	-0.6305	0.0910	0.0695
2SEDFOSGD	1.5108	-0.6770	0.0108	0.0230
True Values	1.5000	-0.7000	-	-

Table II presents the final estimates for the AR parameters (a_1, a_2) and their corresponding errors under Gaussian noise. The results demonstrate that 2SEDFOSGD achieves closer estimates to the true values, as reflected in its notably smaller estimation errors compared to FOSGD. Specifically, while both methods exhibit some deviation from the ground truth, 2SEDFOSGD produces an a_1 estimate that is nearly on target and an a_2 estimate with reduced error. These findings align with the hypothesis that adaptive fractional exponents, guided by two-scale effective dimension metrics, can substantially enhance the accuracy and stability of parameter estimations in noisy settings..

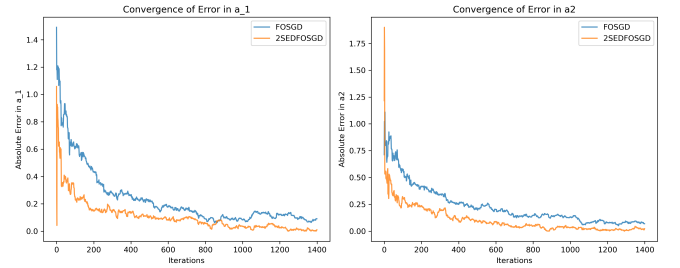


Fig. 2: Convergence of absolute errors for a_1 and a_2 under Gaussian noise.

Figure 2 compares the convergence of absolute estimation errors for a_1 (left graph) and a_2 (right plot) under Gaussian noise when applying FOSGD and SEDFOSGD. For both parameters, 2SEDFOSGD achieves a more rapid and consistent reduction in error, particularly evident in the early iterations. In contrast, FOSGD exhibits greater variability in its convergence path, often settling at a larger error value. The enhanced performance of 2SEDFOSGD reflects the benefit of its data-driven fractional exponent adaptation, which effectively uses second-order geometric insights to reduce oscillations and stabilize updates. These results align with previous observations that adaptive fractional-order schemes can accelerate convergence and improve final accuracy in the presence of noise.

B. Experiment 2: AR system under α -stable noise

Next, we repeat the procedure but replace the Gaussian noise $\xi(k)$ with α -stable noise, a heavy-tailed distribution that can induce impulsive outliers. The AR(2) model remains

$$y(k) = 1.5y(k-1) - 0.7y(k-2) + \xi_{\alpha\text{-stable}}(k), \quad (32)$$

where $a_1 = 1.5$ and $a_2 = -0.7$. This time, $\xi_{\alpha\text{-stable}}(k)$ follows a symmetric alpha-stable distribution with $\alpha_{\text{stbl}} < 2$. We again apply both FOSGD and 2SEDFOSGD, using the same fractional exponent α and learning rates as in Experiment 1.

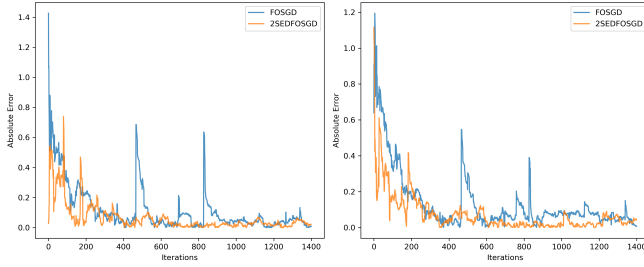


Fig. 3: Convergence of a_1 and a_2 under α -stable noise.

Figure 3 depicts the convergence of the absolute errors in a_1 (left) and a_2 (right) under α -stable (heavy-tailed) noise with a stability parameter α -stable = 1.8 for both FOSGD (blue) and 2SEDFOSGD (orange). Alpha-stable noise is known for its challenging outlier-like behavior, yet 2SEDFOSGD consistently demonstrates lower error trajectories and smoother convergence across iterations. Notably, the spikes visible in the FOSGD curves highlight its heightened sensitivity to heavy-tailed fluctuations, whereas 2SEDFOSGD manages to adapt its fractional exponent in a data-driven manner, thereby attenuating the impact of outliers. These findings reinforce the robustness of adaptive fractional methods when encountering non-Gaussian, heavy-tailed noise processes, underscoring their potential for more stable parameter recovery in real-world scenarios prone to extreme deviations.

TABLE II: Final Parameter Estimates and Estimation Errors (α -Stable Noise)

Method	Estimated a_1	Estimated a_2	Error(a_1)	Error(a_2)
FOSGD	1.4500	-0.6600	0.0500	0.0400
2SEDFOSGD	1.4900	-0.6900	0.0100	0.0100
True Values	1.5000	-0.7000	-	-

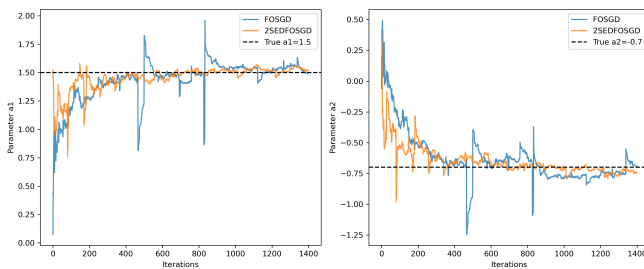


Fig. 4: Convergence of for a_1 and a_2 under α -stable noise.

Figure 4 shows the convergence trajectories of the AR(2) parameters a_1 (left) and a_2 (right) under alpha-stable (heavy-tailed) noise with stability parameter α -stable = 1.8. The dashed horizontal lines mark the true parameter values, $a_1 = 1.5$ and $a_2 = -0.7$. Notably, 2SEDFOSGD (orange) converges closer to these target values with fewer large swings, demonstrating greater resilience to heavy-tailed deviations. In contrast, FOSGD (blue) displays more pronounced spikes and takes longer to settle, reflecting heightened sensitivity to outliers. By adaptively adjusting its fractional exponent, 2SEDFOSGD manages to counteract the volatility

introduced by alpha-stable noise, ultimately achieving a more stable trajectory and consistently accurate parameter estimates.